NeuroImage: Clinical 18 (2018) 730–743

Contents lists available at ScienceDirect

NeuroImage: Clinical

journal homepage: www.elsevier.com/locate/ynicl

"Motoring in idle": The default mode and somatomotor networks are overactive in children and adolescents with functional neurological symptoms

Kasia Kozlowska[a,b,c,*], Chris J. Spooner[d], Donna M. Palmer[b,c], Anthony Harris[b,c,e], Mayuresh S. Korgaonkar[b,c], Stephen Scher[c,f], Leanne M. Williams[g]

[a] The Children's Hospital at Westmead, Psychological Medicine, Locked Bag 4001, Westmead, NSW 2145, Australia
[b] The Brain Dynamics Centre, Westmead Institute for Medical Research, 176 Hawkesbury Rd, Westmead, NSW 2145, Australia
[c] The University of Sydney, Sydney, Australia
[d] Brain Resource, 235 Jones St, Ultimo, NSW 2017, Australia
[e] Westmead Hospital Psychiatry Department, Darcy Rd, Westmead, NSW 2145, Australia
[f] Department of Psychiatry, Harvard Medical School, McLean Hospital, Belmont, MA, USA
[g] Psychiatry and Behavioral Sciences, Stanford University, VA Palo Alto (Sierra-Pacific MIRECC) 401 Quarry Rd, United States

ARTICLE INFO

Keywords:
Functional neurological symptom disorder
Conversion disorder
Functional neurological symptoms
EEG
Dissociation
Glial cells

ABSTRACT

Objective: Children and adolescents with functional neurological symptom disorder (FND) present with diverse neurological symptoms not explained by a disease process. Functional neurological symptoms have been conceptualized as somatoform dissociation, a disruption of the brain's intrinsic organization and reversion to a more primitive level of function. We used EEG to investigate neural function and functional brain organization in children/adolescents with FND.

Method: EEG was recorded in the resting eyes-open condition in 57 patients (aged 8.5–18 years) and 57 age- and sex-matched healthy controls. Using a topographical map, EEG power data were quantified for regions of interest that define the default mode network (DMN), salience network, and somatomotor network. Source localization was examined using low-resolution brain electromagnetic tomography (LORETA). The contributions of chronic pain and arousal as moderators of differences in EEG power were also examined.

Results: Children/adolescents with FND had excessive theta and delta power in electrode clusters corresponding to the DMN—both anteriorly (dorsomedial prefrontal cortex [dmFPC]) and posteriorly (posterior cingulate cortex [PCC], precuneus, and lateral parietal cortex)—and in the premotor/supplementary motor area (SMA) region. There was a trend toward increased theta and delta power in the salience network. LORETA showed activation across all three networks in all power bands and localized neural sources to the dorsal anterior cingulate cortex/dmPFC, mid cingulate cortex, PCC/precuneus, and SMA. Pain and arousal contributed to slow wave power increases in all three networks.

Conclusions: These findings suggest that children and adolescents with FND are characterized by overactivation of intrinsic resting brain networks involved in threat detection, energy regulation, and preparation for action.

1. Introduction

Functional neurological symptom disorder (FND) involves disturbances of body function characterized by neurological sensory or motor symptoms. Patients with FND present with many diverse symptoms not explained by neurological disease, including: psychogenic non-epileptic seizures (PNES); positive movements such as tremor, dystonia, or gait abnormalities; loss of motor functions such as leg or arm paresis; and loss of sensory functions such as blindness, deafness, or loss of feeling in the limbs. Known medical factors do not explain these symptoms or the impairment they confer. In children and adolescents, functional neurological symptoms are generated in the context of pain, injury, intense distress, or psychological trauma, are associated with states of high arousal (Kozlowska et al., 2015a; Kozlowska et al., 2017a;

* Corresponding author at: The Children's Hospital at Westmead, Psychological Medicine, Locked Bag 4001, Westmead, NSW 2145, Australia.
E-mail addresses: kkoz6421@uni.sydney.edu.au, kasia.kozlowska@health.nsw.gov.au (K. Kozlowska), chrissp@iinet.net.au (C.J. Spooner), Donna.palmer@sydney.edu.au (D.M. Palmer), Anthony.Harris@sydney.edu.au (A. Harris), M.Korgaonkar@sydney.edu.au (M.S. Korgaonkar), sscher@mclean.harvard.edu (S. Scher), leawilliams@stanford.edu (L.M. Williams).

https://doi.org/10.1016/j.nicl.2018.02.003
Received 27 November 2017; Received in revised form 19 January 2018; Accepted 2 February 2018
Available online 17 February 2018

Kozlowska et al., 2017b), and are comorbid with medically unexplained pain, nonspecific somatic symptoms, anxiety, and depression (Ani et al., 2013; Kozlowska et al., 2007). Functional neurological symptoms have been conceptualized as somatoform dissociation (Janet, 1889; Janet, 1892/1894; Nijenhuis et al., 1998; Vuilleumier and Cojan, 2011; Barzegaran et al., 2016), which is thought to involve a disruption of the brain's intrinsic organization, and reversion to a more primitive level of neural function (Jackson, 1884)—a brain state where the influence of emotionally salient information on motor output (self-protective reflexive behaviour) is prioritized (Blakemore et al., 2016). Since electroencephalogram (EEG) recordings provide a direct index for quantifying neural function and investigating functional brain organization (Boord et al., 2007; Nagata et al., 1989; Alper et al., 2006), we used EEG to investigate whether functional brain organization is disrupted, at rest, in children and adolescents presenting with acute functional neurological symptoms.

A central idea from evolutionary neuroscience is that functional networks of the brain are organized along a phylogenetic hierarchy that reflects stages in development (Jackson, 1884; MacLean, 1990; Knyazev, 2012; Arnsten, 2015). According to this framework each functional network reflects distinct ways of solving adaptive challenges (Knyazev, 2012; Mesulam, 1998; Buzsaki and Draguhn, 2004; Arnsten, 2015). The particular challenges encountered in any particular situation determine the level of physiological and cortical arousal, the activation state of the brain's innate immune effector cells (glial cells) (Frank et al., 2016), and the functional network that comes into play (Knyazev, 2012; Arnsten, 2015; Hermans et al., 2011; Ding et al., 2013).

States of calm and safety facilitate cognitive/integrative processing, which relies on higher cognitive functions mediated by the prefrontal cortex (PFC), which itself has an executive role in motor planning and motor-control functions—including the inhibition of inappropriate behaviours (Zhang et al., 2012; Knyazev et al., 2017). Such evolutionarily "advanced" processes become operational with maturation and involve activation of cortical brain regions. These processes are associated with the higher-frequency bands (alpha, beta, and gamma) of the EEG (Knyazev, 2007; Knyazev, 2012; Knyazev et al., 2017). By contrast, danger and states of high arousal require emotion and motor-sensory processing; catecholamines impair the higher executive functions of the PFC (Arnsten, 2015; Hermans et al., 2011) and strengthen reflexive control of behaviour (Arnsten, 2015; Hermans et al., 2011). Catecholamines also activate the brain's glial cells, which are more numerous in subcortical versus cortical regions (Mittelbronn et al., 2001), and which function as neuromodulators on a network level, regulating levels of network excitability and resetting basal responsiveness of neural circuits (Ding et al., 2013). Via all these mechanisms, in the face of danger, the brain prioritizes older, more primitive processes—homeostatic defensive functions that include energy regulation, autonomic activity, respiratory rhythms, processing of homeostatic and pain afferents, and activation of innate fear responses and other automatic behaviours—which involve activation of subcortical and limbic structures, and are associated with the low-frequency bands (delta and theta) of the EEG (Knyazev, 2007; Knyazev, 2012).

Evidence from contemporary imaging studies has enabled the identification of the functional networks that are central to the organization of the brain at rest and during task-evoked states (Raichle, 2015; Williams, 2017; Gordon et al., 2016). At rest, the default mode network (DMN), defined by nodes in the medial PFC, posterior cingulate/precuneus cortex, and lateral temporoparietal cortex, is thought to have an important role in self-directed thought and the capacity to switch flexibly into and among alert states (Hagmann et al., 2008; Raichle, 2015). Various mental disorders have already been conceptualized in terms of specific dysfunctions in the DMN (Williams, 2017; Wang et al., 2016), and it is reasonable to assume that disorders of dissociation, including the full spectrum of functional neurological symptoms, will likewise involve disruptions in the DMN.

The DMN is also involved in energy regulation, as is the salience network, the limbic network defined by the anterior insula, dorsal anterior cingulate cortex (ACC), and amygdala (Menon and Uddin, 2010; Williams, 2017). Kleckner et al. (2017) have determined that the default mode and salience networks —operate together as a single, allostatic-interoceptive brain system that maintains energy regulation in the body and that also supports a wide range of psychological functions such as emotion processing, pain processing, memory, and decision making (Kleckner et al., 2017). This allostatic-interoceptive brain system continuously predicts the body's energy needs and uses these predictions to regulate the body's physiological systems to maintain energy regulation in the body (allostasis). In this way, in the face of danger, this system anticipates the body's increased need for energy and activates brain-body systems that enable increased energy consumption. When the danger has passed, the allostatic-interoceptive system changes its predictions and readjusts the energy-regulation system. Activation of the allostatic-interoceptive system is adaptive in the short term but maladaptive in the long term. Continued activation of the system increases the risk for a broad range of stress-related physical and psychological disorders (McEwen and Gianaros, 2011). Accumulating evidence suggests that patients with FND show activation of brain-body systems—the hypothalamic-pituitary-adrenal (HPA) axis, autonomic nervous system, and brain systems underpinning arousal—that mediate increases in arousal and energy consumption (Bakvis et al., 2009a; Bakvis et al., 2009b; Kozlowska et al., 2015a; Apazoglou et al., 2017; Voon et al., 2010). These data suggest that maladaptive activation of the allostatic-interoceptive brain system, together with aberrant activation/disruption of motor systems (Blakemore et al., 2016), may be a core feature of FND.

Functional magnetic resonance imaging (fMRI) studies with adult patients with PNES show overactivation and over- and under-connectivity of the intrinsic organization of the brain at rest. In a study using seed regions, van der Kruijs et al. (2012) showed enhanced connectivity between the insula (part of the salience network) and multiple other seed regions: the central sulcus, posterior cingulate cortex, anterior cingulate cortex, and parietal occipital fissure (van der Kruijs et al., 2012). In a later study, using whole-brain analyses, van der Kruijs et al. (2014) showed increased coactivations in resting-state cortical networks as identified by Smith et al. (2009): increased coactivation of the precuneus and (para-)cingulate gyri in the DMN; increased coactivation of the orbitofrontal, insular, and subcallosal cortex in "fronto-parietal network"; increased coactivation of the cingulate and insular cortex in the "executive control network"; increased coactivation of the cingulate gyrus, superior parietal lobe, pre- and postcentral gyri, and supplemental motor cortex in the "sensorimotor network" (van der Kruijs et al., 2014). With the exception of the default mode and sensorimotor networks (also known as the somatomotor network, the term used in the present study), the networks identified by Smith and taken up by van der Kruijs are not always exactly the same as those identified in other studies (Williams, 2017; Menon and Uddin, 2010).

A resting-state study with adult patients with motor symptoms (both positive and negative) also showed over- and under-connectivity of the intrinsic organization of the brain at rest (Wegrzyk et al., 2017). Changes in regions that define the DMN and in subcortical regions mediating motor and affective functions—increased connectivity between the paracentral lobule and frontal regions (bilateral mid orbital gyri), increased connectivity between the subcortical (right caudate) region and both the limbic (left amygdala) and parietal regions (bilateral postcentral gyri), and decreased connectivity between the parietal regions (right temporoparietal region, including the inferior parietal lobule) and frontal regions (right superior orbito-frontal gyrus)—were most helpful in differentiating patients from healthy controls (Wegrzyk et al., 2017).

Resting-state EEG studies in patients with PNES also suggest changes in cortical function: decreased coherence between frontal and

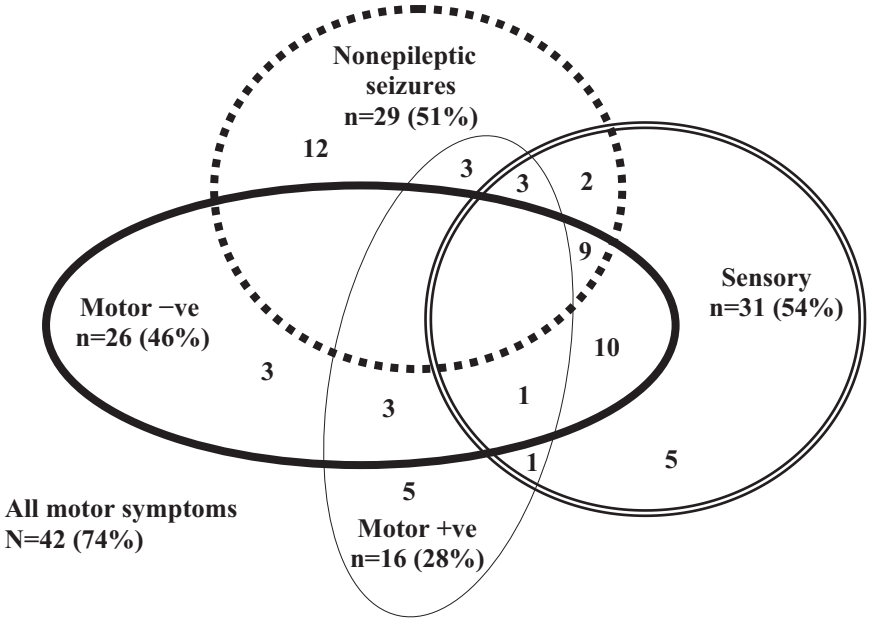

Fig. 1. The visual representation shows the complex patterns of comorbidity between functional neurological symptoms in the current cohort of child and adolescent patients. Non-epileptic seizures commonly presented alongside sensory, positive motor, and negative motor symptoms. Comorbidity between positive and negative motor symptoms was present in four patients: one 11-year-old girl presented with tremor of the right arm alternating with weakness in the right arm and paralysis of both legs; another 11-year-old girl presented with leg weakness alternating with tic-like movements of all four limbs; one 12-year-old boy presented with unremitting cough and weakness in all four limbs; and one 14-year-old boy presented with astasia abasia, leg weakness, voice slurring, and loss of vision.

posterior regions in the gamma band (Xue et al., 2013); changes in EEG synchronization between electrode sites in frontal and posterior (parieto-occipital) regions across power bands, with lower synchronization in frontal regions being related to more frequent PNES (Knyazeva et al., 2011); a disruption of the normal ratio of local and global connectedness in the alpha band (Barzegaran et al., 2012); decreased gamma band source density in the right posterior parietal cortex, posterior cingulate cortex, and superior temporal gyrus (Umesh et al., 2017); and decreased coherence between the right posterior cingulate gyrus and right middle temporal gyrus (Umesh et al., 2017). Another study used the local autoregressive average method and a measure of lagged synchronization to examine connectivity between subcortical and cortical regions. It found weakened functional connectivity between the basal ganglia and the paralimbic, prefrontal, temporal, parietal, and occipital regions (Barzegaran et al., 2016).

In the current study we examined resting-state neural activation within the default mode, salience, and somatomotor networks, quantified by EEG power, in children and adolescents with FND. The salience network and the DMN—the medial prefrontal regions of the DMN, in particular—are activated by interoceptive signals of pain, anxiety, and autonomic arousal (Craig, 2011; Menon and Uddin, 2010; Vachon-Presseau et al., 2016; Raichle, 2015; Teves et al., 2004) and are involved in viceromotor (autonomic) control of allostatic functions, which prepare the body for action (Kleckner et al., 2017). These interoceptive and energy-regulation processes are associated with power increases in the low-frequency bands (Knyazev, 2012). In this context we hypothesized that children and adolescents with FND, who have been found to have high rates of pain, anxiety, and autonomic/cortical arousal (Kozlowska et al., 2015a; Kozlowska et al., 2017b), would show power increases in neural activation in the low-frequency, delta and theta bands and not in the higher-frequency, alpha and beta bands in the default mode, salience, and somatomotor networks. We also investigated which components of the default mode, salience, and somatomotor networks were activated by pain and arousal, and whether such activation was correlated with subjective anxiety, depression, and stress. We assessed the source localization of activation differences in EEG power using low-resolution brain electromagnetic tomography (LORETA).

2. Methods

2.1. Participants

Participants were 57 children and adolescents with functional neurological symptom disorder (41 girls; 16 boys) aged 8.5–18 years (mean: 13.56, SD: 2.2 years) recruited between August 16, 2006, and August 16, 2010, from a paediatric tertiary-care hospital in New South Wales, Australia, as part of a broader research program with the same cohort (Kozlowska and Williams, 2010; Kozlowska et al., 2011; Kozlowska et al., 2013; Kozlowska et al., 2015a; Kozlowska et al., 2015b; Kozlowska et al., 2017b). Twenty-two children were prepubertal (14 girls and 8 boys), and 35 were postpubertal (27 girls and 8 boys). Participants were diagnosed according to modified DSM-IV-TR criteria (AmericanPsychiatric, 2000) by both a paediatrician and a child psychiatrist. Consistent with later-adopted DSM-5 criteria, however, we did not adhere to the DSM-IV-TR "psychological stressor criterion"; our previous research with children/adolescents had highlighted that the psychological-stressor criterion was too narrow (Kozlowska et al., 2007; Kozlowska et al., 2011). Instead, we documented, if present, any antecedent stressors—both psychological and physical. Again, consistent with DSM-5 criteria, all participants had documented positive signs on neurological examination, plus a worsening of symptoms with attention and a decrease of symptoms when distracted by schoolwork and other activities during family assessment, individual assessment, and the inpatient admission.

The participants presented with one or more functional neurological symptoms (mean: 2.60, range: 1–7)—sensory symptoms (n = 31, 54%), motor symptoms (n = 38, 67%), non-epileptic seizures (n = 29, 51%)—that were sufficiently disabling to require hospital treatment in 95% (54/57) of cases (See Fig. 1). At the time of testing, participants were experiencing functional neurological symptoms; that is, the resting EEG was recorded while they were experiencing functional neurological symptoms or during a period of time in which their non-epileptic seizure episodes were occurring. The EEG was recorded soon after the clinical assessment, while all but two patients were medication free (see Kozlowska et al., 2015a for details) (Kozlowska et al., 2015b); of the two adolescents suffering from comorbid neurological disorders, one had epilepsy treated with sodium valproate, and one had a long-standing tremor and a glucose-transporter abnormality treated with sodium valproate plus levetiracetam. Information from school reports

Table 1
Clinical and Demographic information about participants with FND (n = 57).

Socioeconomic status of the family	Number	Percentage
Professional	19	33%
White collar	23	40%
Blue collar	14	25%
Unemployed	1	2%
Antecedent life events (range 1–10, mean 5.3)		
Family conflict	38	67%
Child physical illness	27	47%
Bullying	27	47%
Loss via separation from a loved one or a friend	23	40%
Loss via death of a loved one	19	33%
Maternal mental illness	19	33%
Paternal mental illness	17	30%
Maternal physical illness	15	26%
Moving house	13	23%
Domestic violence events	12	21%
Father mental illness	9	16%
Physical abuse	9	14%
Neglect	6	11%
Sexual abuse	6	9%
Medical investigations		
Physical examination by a paediatrician/paediatric neurologist	57	100%
Blood screen	57	100%
Clinical EEG to exclude epilepsy in patients presenting with PNES/functional movements	32	56%
Brain imaging (MRI, CT or both)	47	83%
ERP/nerve conduction studies	6	11%
Cardiology investigations (ECG, echocardiogram, cardiac telemetry, or tilt-table testing)	9	16%
Intelligence quota estimated from school testing and school reports		
Superior range (120+)	10	18%
Average range (80–119)	43	75%
Borderline range (70–79)	4	7%

and teacher reports (gathered routinely as part of the clinical assessment), as well as, in some cases, past IQ assessments, confirmed that prior to presentation with FND, all patients had being attending school full time, fell within the normal IQ range, and displayed none of the characteristics—history of inattention, impulsivity, behavioural problems, or learning difficulties—that signal maturational delays and an underdeveloped PFC. Additional information about the clinical and demographic characteristics of the patients with FMD is provided in Table 1.

During clinical assessment, all patients with functional neurological symptoms and their families reported antecedent stressors, including physical illness, injury, or pain, and emotional distress or psychological trauma (Table 1)[1]. Assessments of attachment by blinded coders and classification of patients into high-risk, non-normative patterns of attachment confirmed the presence of chronic relational stress (Kozlowska et al., 2011). Using DSM-IV-TR criteria, 54% (31/57) of patients were diagnosed with a comorbid anxiety disorder, 14% (8/57) with depression, and 14% (8/57) with mixed anxiety/depression. Fifty-eight percent (33/57) reported comorbid medically unexplained pain in one (n = 17), two (n = 11), or three sites (n = 5), including 37% (21/57) headache, 23% (13/57) leg pain, 21% (12/57) arm pain, 3% (2/57) body/torso pain, 2/57 (3%) back pain, 2/57 (3%) neck pain, and 2% (1/57) chronic abdominal pain. In addition, 54% (31/57) had comorbid nonspecific somatic symptoms: 14% (8/57) nausea, 30% (17/57) dizziness, 23% (13/57) breathlessness, and 28% (16/57) fatigue. The severity of the child/adolescent's functional impairment was documented using the Royal Alexandra Hospital for Children Global Assessment of Function (RAHC-GAF) (Table 2).

FND participants were compared to 57 healthy children and adolescents matched on age, sex, and years of education, and who completed the same test battery as the clinical sample. Each participant with FND was closely age-matched to ensure an age difference of ≤6 months. Between-group comparisons on the Spot-the-Word test, Depression Anxiety and Stress Scales (DASS), Early Life Stress Questionnaire (ELSQ), and RAHC-GAF confirmed that the FND and control groups were matched on IQ and that the control group was healthy (Table 3).

The study was approved by the institutional ethics committees—Royal Alexandra Hospital for Children (The Children's Hospital at Westmead) Human Research Ethics Committee and Western Sydney Local Health District Human Research Ethics Committee. Written informed consent was obtained from all subjects and their parents. Details on the recruitment protocols, screening for inclusion and exclusion criteria, assessment for organic pathology, and other aspects of clinical characteristics have been reported previously (Kozlowska et al., 2013; Kozlowska et al., 2015a; Kozlowska et al., 2015b; Kozlowska et al., 2011; Kozlowska and Williams, 2010).

2.2. Procedure

Participants' EEGs were recorded in the laboratory during the resting eyes-open condition. Participants were asked to rest quietly, with their eyes open for three minutes. Heart rate was simultaneously recorded via an electrocardiogram (ECG), and skin conductance via electrodes on the left hand. Participants also completed the Spot-the-Word Test (Intelligence Quotient estimate), self-report DASS regarding the presence of emotional symptoms, and ELSQ (Table 2).

2.3. EEG acquisition methodology

EEG was recorded using 26 cephalic sites at Fp1, Fp2, Fz, F3, F4, F7, F8, Cz, C3, C4, FC3, FCz, FC4, T3, T4, T5, T6, Pz, P3, P4, O1, O2, and Oz electrode sites (10–20 International System). A QuickCap (Neuroscan) was used to acquire EEG data from these cephalic sites. EEG data were referenced to the average of A1 and A2 (mastoid) electrodes sites. For the horizontal electrooculogram (EOG), horizontal eye movements were recorded with electrodes placed 1.5 cm lateral to the outer canthus of each eye. Vertical eye movements were recorded with electrodes placed 3 mm above the middle of the left eyebrow and 1.5 cm below the middle of the left bottom eyelid. Skin resistance was kept at < 5 kΩ. Scalp, EOG, and other potentials were amplified and digitized continuously by a system (NuAmps, SCAN 4.3) having a frequency response from DC to 100 Hz (above which, attenuating by 40 dB per decade), a sampling rate of 500 Hz, and a 22-bit resolution digitization. Correction for eye-blink artifact was carried out on the 26 cephalic sites using a technique based on Gratton et al. (1983) (Gratton et al., 1983) using the recorded EOG data. The Brain Resource database software was used to perform artifact handling on the EEG. Epochs are rejected if the signal at three or more sites exceeded 100 μV voltage swing for that particular epoch.

2.4. Arousal measures

An electrocardiogram (ECG)—yielding heart rate (HR) and heart

[1] The rates of sexual abuse are higher than previously reported due to subsequent disclosures. In the child physical illness/injury category, accidental injury and viral illnesses were the most common.

Table 2
Summary self-report and clinician-report measures used in the study.

Self-report and Clinician Report Measures	
RAHC-GAF	The Royal Alexandra Hospital for Children Global Assessment of Function (RAHC-GAF) is the DSM-IV-TR GAF modified to include functional impairment secondary to physical illness (AmericanPsychiatric, 2000). The scale has 100 points and 10 categories (10 points each). Healthy controls fall into the upper two brackets "superior in all areas (score 91–100) or "good in all areas (score 81–90). Lower values (and brackets) mark functional impairment of increasing severity. Patients with physical or psychological impairment fall into the lower brackets (score < 81).
Spot-the-word test (IQ estimate)	The spot-the-word test is an IQ estimate. Subjects are presented with pairs of items comprising one word and one non-word, and requiring the subject to identify the word (Baddeley et al., 1993; Hatch et al., 2010). Performance correlates highly with verbal intelligence and in adult's correlates with performance on the National Adult Reading Test (NART).
DASS-21	The Depression Anxiety and Stress Scales are in paediatric populations is a validated measure of perceived distress in paediatric populations (Lovibond and Lovibond, 1995; Patrick et al., 2010).
ELSQ	The early life stress questionnaire (ELSQ) is a checklist of 19 stress items—and an option for elaboration—based on the Child Abuse and Trauma Scale (Cohen et al., 2006). Twelve items pertained to stress from repeated relational stressors including: bullying; physical abuse; sexual abuse; emotional abuse; neglect; parental separation; loss by separation; loss by death; family conflict; severe illness of a family member; domestic violence; repeated illness/hospitalizations and other. Other items pertain to birth complications, war trauma, natural disasters and life threatening illness. Participants record if they have or have not experienced the given stressor and the age period during which the stressor has been experienced.

Table 3
Comparisons between FND and healthy-control groups on IQ and self-report.

Measure	FND group mean value/total score	Healthy-control group mean value/total score	t/χ^2 (p)
Spot-the-word test (IQ estimate)	39.58	38.59	0.75 (0.45)
DASS-21 total score	11.49	4.52	4.56 (< 0.001)
DASS stress subscale	4.53	2.15	3.91 (< 0.001)
DASS anxiety subscale	3.91	1.25	4.60 (< 0.001)
DASS depression subscale	3.05	1.34	2.85 (0.006)
ELSQ relational-stressors (number marked)	121/498 items	69/672 items	41.39 (< 0.001)
RAHC-GAF	38 (range 11–75)	> 80*	22.64 (< 0.001)

For the t-test analysis healthy controls were assigned the arbitrary value of 81.

rate variability (HRV) measures (see Kozlowska et al., 2015a for details regarding ECG methodology)—and skin-conductance measures were acquired simultaneously with the EEG recording. Skin conductance was recorded with the same frequency response, sampling rate, and resolution as the EEG data. The slope of the change in skin-conductance level (in microsiemens/s) across a given recording was calculated.

2.5. EEG Spectral power methodology

Each 2-min EEG recording was partitioned into 4096-millisecond, 50% overlapping epochs. Each epoch is windowed using a Welch window before Fast Fourier Transform (FFT) is applied. Average power spectra were computed for 58 epochs of FFT for the eyes-open condition. Bad channels were excluded by inspection. Epochs with maximal voltage-swing values over 100 uV on at least three channels were excluded. The spectral power was calculated for four bands: delta (1.5–3.5 Hz), theta (4–7.5 Hz), alpha (8–13 Hz), and beta (14.5–30 Hz).

2.6. EEG spectral power analysis

In the EEG power data, outliers beyond 2.5 standard deviations were removed, and missing values were replaced with the group mean, determined separately for children aged < 12 years and ≥12 years in both the FND and control groups (Tabachnick and Fidell, 2007). Logarithmic transformation was applied to ensure that all EEG data approximated a normal distribution.

EEG power data were quantified for regions of interest that define the default mode, salience, and somatomotor networks. The DMN was defined according to the topographical map developed by Giacometti et al. (2014) (Giacometti et al., 2014). The regions of the anterior DMN (and the corresponding EEG sites) included the ventromedial prefrontal cortex cluster (vmPFC; Fp1, Fp2), dorsomedial prefrontal cortex cluster (dmPFC; Fz, Cz), and rostral anterior cingulate cortex cluster (rostral ACC; Fp1, Fz, F4, Fp2)[2]. Regions of the posterior DMN (and the corresponding EEG sites) included the posterior cingulate cortex cluster (PCC; Cz, C4), precuneus cluster (O1, Pz, O2), and lateral parietal region adjacent to the temporal lobe cluster (P3, P4).

The salience network was defined according to two core regions within the network (Seeley et al., 2007; Williams, 2017; Touroutoglou et al., 2014): the insula cluster (F7, F8, T6) and the dorsal ACC cluster (Fz, F4).

The somatomotor network was defined according to the core region within the network (Williams, 2017), the premotor/supplementary motor area (SMA) (FC3, FC1, FCZ, FC2, FC4) (Puzzo et al., 2010)[3].

Repeated measures ANOVAs were used to examine differences between the FND and controls groups for these default mode, salience, and somatomotor regions of interest for the two slow-wave power bands (delta and theta) and two fast-wave power bands (alpha and beta).

2.7. Pain as a moderator

The contribution of chronic pain as a moderator of FND-related differences in EEG power in the default mode, salience, and somatomotor networks was examined using repeated measures ANOVAs, with FND participants stratified by characteristics of pain versus controls. Planned contrasts were undertaken using the Least Significant Difference Test.

[2] The rostral ACC includes the perigenual and subgenual ACC, which are considered to be part of the DMN.

[3] We utilized coordinates equivalent coordinates FC3, FCz and FC4 because our system did not provide us with readings for FC1 and FC2.

2.8. Arousal as a moderator

The contribution of arousal as a moderator of FND-related differences in EEG power in the default mode, salience, and somatomotor networks was examined by rerunning the repeated measures ANOVAs with the three indices of arousal—RMSSD-HRV,[4] HR, and skin-conductance level as separate covariates at sites showing significant or trend-level between-group differences. Missing values for RMSSD-HRV, HR, and skin conductance were replaced with the group mean, determined separately for children aged < 12 years and ≥12 years in both the FND and control groups (Kozlowska et al., 2015a).

2.9. Symptom correlates

Within the FND group, we examined the correlation between symptoms of subjective distress (the total score from the DASS[5]), functional impairment, (GAF) and EEG cluster variables that showed significant between-group differences. Participants with missing DASS scores were omitted from the analysis.

2.10. Source-localization analysis

In order to implement source-localization analysis in sLORETA (KEY institute http://www.uzh.ch/keyinst/loreta.htm), the EEG recording was partitioned into 2048-millisecond epochs. The same epoch and channel-exclusion methods as per spectral scoring were applied. If any given channel had less than three adjacent channels, then the data for that subject was excluded altogether. Otherwise, spherical spline interpolation based on neighbouring channel data was used to interpolate channel data missing due to artifacts. The sLORETA software was used to compare the FND group to controls. Source localization was undertaken within each of the EEG frequency bands used for the spectral power analysis. Logarithmic transformation was applied to ensure that all data approximated a normal distribution. A single head model was used (as provided by the KEY institute sLORETA software). We identified the group differences in peak activity defined by regions with maximal voxels, using a whole-brain approach. The LORETA method yields a t-critical value that is effective for controlling type I error.

2.11. Post hoc analyses examining developmental (age-related) characteristics and power differences in a "control network"

Because the age range of the sample was very large, two post hoc analyses were run to examine whether our EEG data were robust and conformed with developmental and neurophysiological characteristics previously-described in the broader literature. The first post hoc analysis examined whether the data showed a reduction of slow waves (a decrease in the power ratio index [PRI]) with maturation. Whole-brain PRI values were calculated by dividing the combined delta power and theta power by the combined alpha power and beta power from all sites. Independent sample *t*-tests were used to assess differences in whole-brain PRI between the prepubertal and postpubertal participants within the FND and controls groups.

The second post hoc analysis—a rerun of (significant) ANOVA analyses in electrode clusters in the whole-group analysis, by pubertal status—to eliminate the possibility that whole group differences were age-related or driven by pubertal status. A chi-square analysis was used to compare the number of significant and non-significant results in the prepubertal versus postpubertal groups.

The third post hoc analysis examined whether our data showed the normal robust relationship between HRV and delta power reported by Jurysta et al. (2003) by running correlations between the time domain measure of HRV (RMSSD-HRV) and the average delta and theta power value at the Cz site (Jurysta et al., 2003).

The fourth post hoc analysis examined between-group differences in a "control network": the cognitive-control network (Williams, 2017). We chose the cognitive-control network—defined according to the core region within the network, the dorsolateral PFC—because this region of the brain would hypothetically not be activated by a functional shift from cognitive/integrative processing to emotion and motor-sensory processing.

3. Results

3.1. Examination of the data

Examination of the data revealed adequate EEG data sets, with 2.65% and 2.63% missing data for FND participants and control participants, respectively. Missing data for RMSSD-HRV (14% and 19%), HR (14% and 14%), skin conductance (2% and 3.5%), and DASS (24.6% and 0%) were higher for some measures. All data approximated a normal distributions (skewness ≤1.11 for EEG clusters; ≤1.14 for arousal data; and 1.00 for DASS).

3.2. Group differences in EEG spectral power analysis in regions of the default mode, salience, and somatomotor networks

Patients with FND showed increased power in both the delta band (dmPFC, PCC, and precuneus electrode clusters) and theta band (dmPFC, PCC, precuneus, and lateral parietal cortex electrode clusters) of the DMN (see Table 4).

Patients with FND also showed increased power in the delta and theta bands in the premotor/SMA electrode cluster (see Table 4).

Power increases in the salience network were evident at the trend level (dorsal ACC cluster in the delta band and insula cluster in the theta band).

By contrast, there were no significant differences in electrode clusters corresponding to the default mode or somatomotor network in either the alpha or beta band (see Table 5).

3.3. Pain and arousal as moderators of group differences in EEG spectral power analysis within regions of the default mode and somatomotor networks

Patients with FND (vs. healthy controls) were characterized by increased autonomic arousal as reflected by higher HR ($t(107) = 4.26$, $p < 0.001$), lower HRV ($t(105) = -2.55$, $p = 0.012$) (Kozlowska et al., 2015a), and increased skin conductance ($t(112) = 2.26$, $p = 0.025$). Patients with FND and pain (vs. patients with FND without pain) were characterized by higher HR at a trend significance level (HR of 84 bpm vs. 80 bpm, $t(55) = 1.776$, $p = 0.081$). Otherwise, there were no differences between FND patients with pain and without pain in terms of age ($t(55) = 0.304$, $p = 0.762$), sex ($\chi^2 = 1.83$, df = 1, $p = 0.18$), pubertal status ($\chi^2 = 0.16$, df = 1, $p = 0.68$), total DASS score ($t(27.683) = 0.641$, $p = 0.527$), RMSSD ($t(55) = 1.027$, $p = 0.309$), and skin conductance ($t(55) = 0.108$, $p = 915$)).

Pain was a moderator of the comparatively increased delta and theta power observed in the patient group in the default mode, salience and somatomotor networks (see Table 6). These findings were strongest for the PCC and precuneus clusters of the DMN in the delta power range. Arousal (indexed by HR) was a moderator of comparatively increased delta power in specific nodes of the DMN (dmPFC, PCC, precuneus, and lateral parietal electrode clusters) the salience network (dorsal ACC) and the somatoform network (SMA) (see Table 7). Arousal (indexed by HR) was also a moderator of comparatively increased theta

[4] RMSSD-HRV = root mean squared successive differences of the interbeat intervals, the time-domain component of HRV measured in ms^2.

[5] The DASS has been validated for use in children and adolescents for total score, but not to distinguish between anxiety, depression, and stress Patrick J, Dyck M and Bramston P. (2010) Depression anxiety stress scale: is it valid for children and adolescents? *Journal of clinical psychology* 66: 996–1007.

Table 4
Differences between FND and control group across ROI in the slow-wave bands.

Site	Mean value FND group across sites log (μV^2)	Mean value control group across sites log (μV^2)	F	df	p-value[a]	Cohen's d effect size
Eyes-open delta power band						
vmPFC cluster	1.49	1.47	0.191	1, 112	0.663	0.09
dmPFC cluster	1.60	1.53	4.375	1, 112	**0.039**	0.40
Rostral ACC	1.53	1.48	1.354	1, 112	0.247	0.22
PCC cluster	1.60	1.48	5.576	1, 112	**0.020**	0.44
Precuneus cluster	1.50	1.40	6.736	1, 112	**0.011**	0.50
Lateral parietal cluster	1.51	1.45	3.385	1, 112	0.068	0.35
Insula	1.37	1.33	0.711	1, 122	0.401	0.16
Dorsal ACC	1.56	1.50	3.624	1, 122	0.060	0.36
Premotor/SMA cluster	1.57	1.49	4.615	1, 112	**0.034**	0.41
Eyes-open theta power band						
vmFPC cluster	1.21	1.15	1.882	1, 112	0.173	0.26
dmPFC cluster	1.50	1.41	4.543	1, 112	**0.035**	0.40
Rostral ACC cluster	1.32	1.25	2.603	1, 112	0.109	0.31
PCC cluster	1.45	1.36	4.892	1, 112	**0.029**	0.42
Precuneus cluster	1.28	1.18	5.189	1, 112	**0.025**	0.43
Lateral parietal cluster	1.36	1.26	4.387	1, 112	**0.038**	0.40
Insula cluster	1.12	1.04	3.502	1, 112	0.064	0.35
Dorsal ACC cluster	1.14	1.13	0.166	1, 112	0.684	0.06
Premotor/SMA cluster	1.45	1.36	4.625	1, 112	**0.034**	0.41

[a] Significant values for $p < 0.05$ are printed in bold.

Table 5
Differences between FND and control group across ROI in the fast-wave bands.

Site	F	df	p-value[a]
Eyes-open alpha power band			
vmPFC cluster	0.110	1, 112	0.741
dmPFC cluster	0.022	1, 112	0.882
Rostral ACC	0.008	1, 112	0.931
PCC cluster	0.218	1, 112	0.642
Precuneus cluster	0.206	1, 112	0.650
Lateral parietal cluster	0.028	1, 112	0.860
Insula cluster	0.002	1112	0.963
Dorsal ACC cluster	0.022	1112	0.882
Premotor/SMA cluster	0.071	1, 112	0.791
Eyes-open beta power band			
vmFPC cluster	1.553	1, 112	0.251
dmPFC cluster	0.092	1, 112	0.762
Rostral ACC	0.908	1112	0.343
PCC cluster	1.064	1, 112	0.305
Precuneus cluster	0.622	1, 112	0.432
Lateral parietal cluster	0.301	1, 112	0.584
Insula cluster	0.463	1112	0.497
Dorsal ACC cluster	0.166	1112	0.684
Premotor/SMA cluster	0.398	1, 112	0.529

power in the insula node of the salience network (See Table 7).

3.4. Source localization

Whole-brain LORETA source localization identified the peak activations in all three networks: the mid cingulate cortex (MCC) (−5 0 40, theta band) and PCC/precuneus (0–60 15, delta band) in the DMN; the dorsal ACC/dmPFC (5 25 40, alpha band) in the salience network; and the left SMA (−25–15 50, beta band) in the somatomotor network (see Fig. 2 and Table 8).

3.5. Correlations with subjective distress and functional impairment

Within the FND group, at the $p = 0.05$ level of significance, there were negative correlations between EEG power in the theta band and subjective distress (total DASS score) in regions of the default mode network (dmPFC cluster, $r(43) = -0.303$, $p = 0.048$; PCC cluster, $r(43) = -0.336$, $p = 0.027$) and somatomotor network (SMA cluster, $r(43) = -0.321$, $p = 0.031$). There were no correlations between EEG power in the delta band and either subjective distress or level of functional impairment (RAHC-GAF score).

3.6. Conformity with known developmental and neurophysiological characteristics, role of pubertal status, and examination of power differences in a control network

Whole-brain PRI in prepuberbal and postpubertal participants showed the expected developmental shift involving a reduction of slow waves (a decrease in PRI) with maturation in both the patient and controls groups (See Table 9). Prepubertal participants with FND had significantly higher whole-brain PRIS than prepubertal healthy controls (mean 2.0 vs. 1.5; $t(30.14) = 2.46$, $p = 0.02$), whereas the increase in PRI ratio in postpubertal participants was not significant (mean 1.3 vs. 1.2; $t(68) = 0.74$, $p = 0.46$). Despite this, a rerun of repeated measures analyses in electrode clusters that were significant in whole-group results in the prepubertal and postpubertal subgroups showed that findings remained significant in 4/9 prepubertal analyses and 2/19 postpubertal analyses, and that between-group findings were not driven by pubertal status ($\chi^2 = 1.00$, df = 1, $p = 0.31$).

Although both patient (Pearson correlation 0.257, $p = 0.053$) and control participants (Pearson correlation 0.438, $p = 0.001$) showed the normative pattern of relationship between RMSSD-HRV and delta power at Cz as previously established by Jurysta et al. (2003) (Jurysta et al., 2003)—that is, as RMSSD-HRV increased, delta power increased—these findings were much stronger in the control versus FND group.

Examination of between-group differences in the cognitive-control network (dorsolateral PFC cluster)—the "control network"—showed no differences in any of the power bands (alpha [$F(1, 112) = 0.004$, $p = 0.95$]; beta [$F(1, 112) = 0.570$, $p = 0.5$]; theta [$F(1, 112) = 2.309$, $p = 0.13$]; and delta [$F(1, 112) = 0.244$, $p = 0.62$].

4. Discussion

In this study we used a topographical map to quantify EEG power data in children and adolescents with functional neurological symptoms (vs. age- and sex- matched healthy controls) in the resting-state, eyes-open condition for regions of interest that define the default mode, salience, and somatomotor networks. Patients with FND had excessive theta and delta power in EEG electrode clusters that correspond to DMN sub-networks both anteriorly (dorsomedial PFC) and posteriorly

Table 6
Differences between FND participants with pain, FND participants without pain, and controls.

Site	Mean value pain-FND group across sites log(μV^2)	Mean value nonpain-FND group across sites log(μV^2)	Mean value control group across sites log(μV^2)	F	df	p-value[a]	Cohen's d effect size
Eyes-open delta power band							
dmPFC cluster	1.62	1.56	1.52	2.873	2111	0.061	0.45
Post hoc LSD analyses showed significant differences only between the pain-FND and control group, $p = 0.$**018**.							
PCC cluster	1.59	1.54	1.48	3.283	2111	**0.041**	0.48
Post hoc LSD analyses showed significant differences only between the pain-FND and control group, $p = 0.$**013**.							
Precuneus cluster	1.53	1.47	1.40	4.030	2111	**0.020**	0.45
Post hoc LSD analyses showed significant differences only between the pain-FND and control group, $p = 0.$**006**.							
Lateral parietal cluster	1.53	1.50	1.45	1.874	2, 111	0.158	0.37
Post hoc LSD analyses showed trend-level differences only between the pain-FND and control group, $p = 0.$**061**.							
Dorsal ACC cluster	1.58	1.54	1.50	2.253	2, 111	0.110	0.40
Post hoc LSD analyses showed significant differences only between the pain-FND and control group, $p = 0.$**037**.							
Premotor/SMA cluster	1.58	1.54	1.49	2.567	2111	0.081	0.43
Post hoc LSD analyses showed significant differences only between the pain-FND and control group, $p = 0.$**029**.							
Eyes-open theta power band							
dmPFC cluster	1.52	1.47	1.41	2.637	2, 111	0.076	0.43
Post hoc LSD analyses showed significant differences only between the pain-FND and control group, $p = 0.$**025**.							
PCC cluster	1.47	1.42	1.36	2.931	2111	0.057	0.46
Post hoc LSD analyses showed significant differences only between the pain-FND and control group, p = **0.018**.							
Precuneus cluster	1.30	1.26	1.18	2.686	2111	0.073	0.44
Post hoc LSD analyses showed significant differences only between the pain-FND and control group, $p = 0.$**031**.							
Lateral parietal cluster	1.36	1.34	1.25	2.215	2111	0.114	0.40
Post hoc LSD analyses showed trend-level differences only between the pain-FND and control group, $p = 0.056$.							
Insula cluster	1.15	1.08	1.04	2.365	2, 111	0.099	0.41
Post hoc LSD analyses showed significant differences only between the pain and control group, $p = 0.$**032**.							
Premotor/SMA cluster	1.47	1.41	1.36	2.750	2111	0.068	0.44
Post hoc LSD analyses showed significant differences only between the pain and control group, $p = 0.$**022**.							

[a] Significant values are printed in bold.

(posterior cingulate cortex, precuneus, and lateral parietal cortex), and excessive theta and delta power in the premotor/SMA electrode cluster, which corresponds to part of the somatomotor network. There was also a trend toward excessive theta and delta power in the salience network (insula and dorsal ACC electrode clusters, respectively). Source-localization analysis provided convergent evidence for the neural sources of these EEG power increases in regions of the default mode, salience and somatomotor networks, with peak activations in the dorsal ACC, MCC, PCC/precuneus and SMA. Source localization using LORETA also suggested that power increases were not restricted to delta and theta, but occurred across power bands. Interoceptive signals of pain contributed to theta and delta power increases in all three networks, with the strongest findings for the PCC and precuneus clusters of the DMN in the delta power range. Arousal contributed to delta increases in all three networks and to theta increases in the insula node of the salience network. Our data suggest that child and adolescent patients with FND show increased activation of the brain at rest in electrode clusters that correspond to the DMN (which is typically activated in the resting state), salience network (which is activated by threat and emotionally salient stimuli), and somatomotor network (typically deactivated, rather than hyperactivated, in the resting state), marking a shift in resting-state functional brain organization.

Based on neuroimaging and neurophysiological studies from the past decade, contemporary models of FND suggest that in patients with FND, brain regions involved in arousal, motivation, emotion processing, and self-referential functions—e.g., the amygdala, cerebellar vermis, vmPFC, and precuneus—respond to aversive and emotionally salient stimuli in an overly robust way, setting the stage for aberrant emotion-motor interactions and the disruption of voluntary motor function (Voon, 2014; Vuilleumier, 2014; van der Kruijs et al., 2014; Blakemore et al., 2016). Along the same lines, resting-state studies looking at intrinsic resting-brain function in patients with FND have documented changes in functional network organization in regions that define the default mode and salience networks and that mediate motor and affective functions (Wegrzyk et al., 2017; van der Kruijs et al., 2012; van der Kruijs et al., 2014). In this context the current findings of power increases within electrode clusters corresponding to the DMN, salience network, and SMA point to altered intrinsic resting (functional) organization—activation of the allostatic-interoceptive-motor brain system—a functional shift to a more defensive brain organization. This form of functional organization is associated with a state of increased vigilance and arousal, a brain state that prioritizes reflexive and emotionally salient, rather than voluntary, modes of motor control and that enables the individual to respond to threat rapidly and automatically (Knyazev, 2007; Knyazev, 2012; Arnsten, 2009). Hypothetically, in susceptible individuals, this form of “defensive” functional organization, in the presence of further stresses or triggers, can incidentally activate aberrant emotion-motor interactions and generate functional neurological symptoms (Kozlowska, 2017).

As previously noted, the DMN plays a central role in the brain's ongoing (intrinsic) activity during the resting state (Raichle et al., 2001). Together with the salience network, the DMN is part of the allostatic-interoceptive brain system, which continually anticipates the body's energy needs and prepares to meet those needs—by activating the body's arousal systems—to ready the body for action (Kleckner et al., 2017). Alongside this interoceptive, energy-regulation function, the DMN supports intrinsic processes pertaining to emotion processing. Within the DMN, the vmPFC processes interoceptive and sensory threat signals and is involved in visceromotor output; the dmPFC is involved in self-referential mental activity; and the posterior cingulate cortex, adjacent precuneus, and lateral parietal cortex are involved in processing emotional salience, representing agency, and recollecting prior experiences (Vachon-Presseau et al., 2016; Raichle, 2015; Teves et al., 2004). The SMA, which is situated in the dmPFC, is part of both the dmPFC region that regulates self-referential information and the cortico-striato-thalamo-cortical circuit motor system, which regulates

Table 7
Differences between FND and control group in the delta and theta bands in the eyes-open condition in sites with significant/trend-level differences, with HRV, HR, and skin conductance run as a covariate.

Site	Mean value FND group across sites log(μV^2)	Mean value control group across sites log(μV^2)	F	df	*p*-value	Cohen's d effect size
Eyes-open delta power band (HRV arousal as a covariate)						
dmPFC cluster	1.60	1.52	8.607	1, 111	0.004	0.56
PCC cluster	1.60	1.48	10.675	1, 111	0.001	0.62
Precuneus cluster	1.50	1.40	11.041	1, 111	0.001	0.63
Lateral parietal cluster	1.51	1.45	6.648	1111	0.011	0.49
Dorsal ACC cluster	1.56	1.50	7.291	1, 111	0.008	0.51
Premotor/SMA cluster	1.57	1.49	9.636	1, 111	0.002	0.59
Eyes-open theta power band (HRV arousal as a covariate)						
dmPFC cluster	1.50	1.41	9.271	1, 111	0.003	0.58
PCC cluster	1.45	1.36	10.506	1, 111	0.002	0.61
Precuneus cluster	1.28	1.18	10.317	1, 111	0.002	0.61
Lateral parietal cluster	1.36	1.26	9.990	1, 111	0.002	0.60
Insula cluster	1.12	1.04	6.861	1, 111	0.010	0.50
Premotor/SMA cluster	1.45	1.36	9.585	1, 111	0.002	0.59
Eyes-open delta power band (HR as a covariate)						
dmPFC cluster	1.60	1.53	2.611	1, 111	**0.109**[a]	0.31
PCC cluster	1.60	1.53	3.151	1, 111	**0.079**[a]	0.34
Precuneus cluster	1.50	1.40	2.931	1, 111	**0.090**[a]	0.33
Lateral parietal cluster	1.51	1.45	1.824	1, 111	**0.180**[a]	0.26
Dorsal ACC cluster	1.56	1.50	2.225	1, 111	**0.139**[a]	0.29
Premotor/SMA cluster	1.57	1.49	2.743	1, 111	**0.100**[a]	0.31
Eyes-open theta power band (HR as a covariate)						
dmPFC cluster	1.50	1.41	4.211	1, 111	0.043	0.39
PCC cluster	1.45	1.36	5.341	1, 111	0.023	0.44
Precuneus cluster	1.28	1.18	4.365	1, 111	0.039	0.40
Lateral parietal cluster	1.36	1.26	5.165	1, 111	0.025	0.43
Insula cluster	1.12	1.04	2.343	1, 111	**0.129**[a]	0.29
Premotor/SMA cluster	1.45	1.36	4.271	1, 111	0.041	0.39
Eyes-open delta power band (skin conductance as a covariate)						
dmPFC cluster	1.60	1.53	4.004	1, 111	0.048	0.38
PCC cluster	1.60	1.48	5.102	1, 111	0.026	0.43
Precuneus cluster	1.50	1.40	5.953	1, 111	0.016	0.46
Lateral parietal cluster	1.51	1.45	2.798	1, 111	0.097	0.32
Dorsal ACC cluster	1.56	1.50	3.493	1, 111	0.064	0.36
Premotor/SMA cluster	1.57	1.49	4.256	1, 111	0.041	0.39
Eyes-open theta power band (skin conductance as a covariate)						
dmPFC cluster	1.50	1.41	4.838	1, 111	0.03	0.42
PCC cluster	1.45	1.36	5.710	1, 111	0.019	0.45
Precuneus cluster	1.28	1.18	5.244	1, 111	0.024	0.43
Lateral parietal cluster	1.26	1.36	4.818	1, 111	0.030	0.42
Insula cluster	1.12	1.04	3.475	1, 111	0.065	0.35
Premotor/SMA cluster	1.45	1.36	5.192	1, 111	0.025	0.43

[a] Values denoting a significant change in the p-value from significant/trend-level (shown in Table 4) to not significant (this Table)—with reanalysis that included the covariate—are printed in bold. These bolded values mark the conditions where the covariate contributed to delta and theta power increases.

skeletomotor control. In its dual role, the SMA has been implicated in the multiple functions of error detection, decision uncertainty, and feedback regarding unfavourable outcomes, as well as in motor initiation, motor inhibition, and the subjective urge to move (Fried et al., 1991; Nachev et al., 2008; Haggard, 2008; Zhang et al., 2012). Increased activation of the DMN, salience networks and SMA, including their generator regions, in the resting state suggests that the brain-body state of child and adolescent patients with FND is characterized by upregulation of emotion-processing regions in the DMN/salience network and motor-processing regions in the SMA. The consequence is a brain-body state with all systems turned on: heightened attention and sensory processing (hypervigilance) along with both visceromotor activation (arousal) and skeletomotor activation (motor readiness). This brain-body state is charged with energy—motoring in idle and ready to go.

We found that subjective pain contributed to theta and delta power increases in the default mode, salience, and somatomotor networks, that arousal (indexed by HR) contributed delta power increases in all three networks and to theta power increases in the salience network, and that patients with FND and pain had higher HRs than those without pain. Taken together, these findings suggest a complex relationship between the pain, distress, visceromotor (arousal), and skeletomotor systems. Whereas pain always activates the sympathetic nervous system (Schlereth and Birklein, 2008), short-term increases in sympathetic activation in healthy individuals suppress pain, and longer-term increases in sympathetic activation augment pain and facilitate the transition to chronic pain (Schlereth and Birklein, 2008). The specific mechanisms through which pain is augmented include the following: catecholamine-mediated sensitization of pain receptors (Janig and Habler, 2000); activation of immune/inflammatory cells into a defensive, pain-enhancing mode of function (Milligan and Watkins, 2009; Ji et al., 2016); and neuroplastic changes both in peripheral spinal cord pain circuits and in brain networks involved in pain processing (Vachon-Presseau et al., 2016; Kuner and Flor, 2017). In parallel, priming of the brain's innate immune/inflammatory effector cells (glial cells) by past, and especially by chronic, stress may help maintain increased activation of the brain at rest and a shift of balance toward low frequencies (Fields, 2009; Frank et al., 2016; Brenhouse and Schwarz, 2016; von Bernhardi et al., 2016).

There was also a weak negative correlation between ratings of

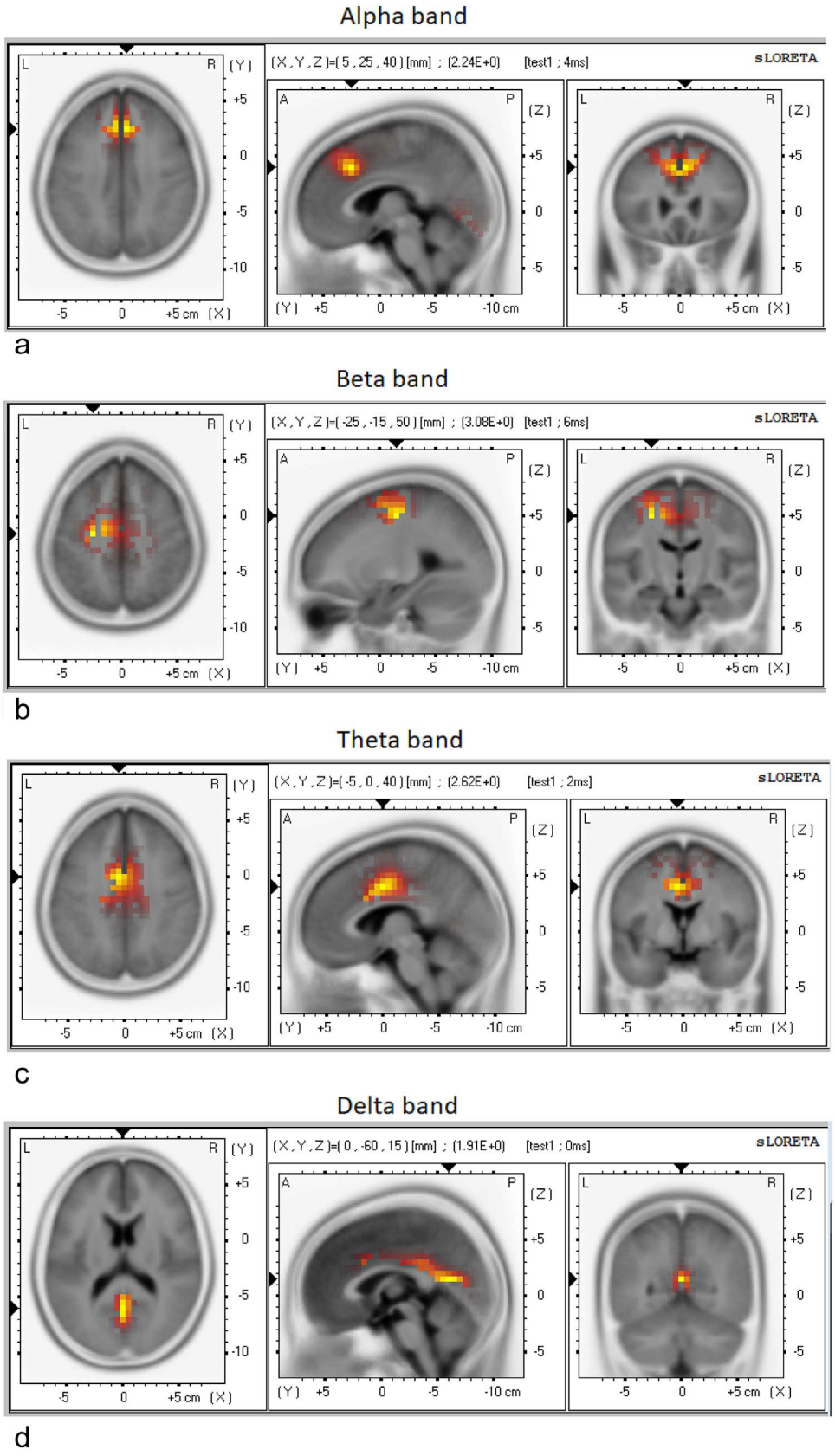

Fig. 2. LORETA source localization shows peak activation in the DMN (PCC/precuneus in the delta band and the MCC in the theta band), the salience network (dorsal ACC/dmPFC in the alpha band) and the somatomotor network (left SMA in the beta band).

Table 8
Significant and trend-level differences between FND and control groups across ROI in the slow and fast wave bands using LORETA analysis.

Site	MNI coordinates	t-value	p-value	Cohen's d effect size
Eyes-open delta power band				
Left rostral ACC	−5, 34, 28	1.54	0.070	0.30
Right rostral ACC	5, 34, 28	1.55	0.062	0.30
Right PCC	10, −58, 14	1.82	0.036	0.35
Left dorsal ACC	−5, 14, 42	1.54	0.063	0.30
Right dorsal ACC	5, 14, 42	1.66	0.050	0.32
Left premotor/SMA	−6, −19, 60	1.19	0.057	0.23
Eyes-open theta power band				
Anterior dmPFC	0, 48, 38	1.79	0.038	0.35
Posterior dmPFC	−2, 7, 50	2.42	0.009	0.47
Left rostral ACC	−5, 34, 28	1.86	0.033	0.36
Right rostral ACC	5, 34, 28	1.85	0.033	0.36
Left PCC	−12, −59, 11	1.77	0.040	0.34
Right PCC	10, −58, 14	2.12	0.018	0.43
Left dorsal ACC	−5, 14, 42	2.42	0.009	0.44
Right dorsal ACC	5, 14, 42	2.45	0.008	0.44
Left premotor/SMA	−6, −19, 60	2.24	0.014	0.44
Right premotor/SMA	5, −19, 60	2.17	0.016	0.42
Eyes-open alpha power band				
Anterior dmPFC	0, 48, 38	1.93	0.028	0.37
Posterior dmPFC	−2, 7, 50	1.93	0.028	0.37
Left rostral ACC	−5, 34, 28	1.96	0.026	0.38
Right rostral ACC	5, 34, 28	1.89	0.030	0.37
Left PCC	−12, −59, 11	1.59	0.060	0.31
Right PCC	10, −58, 14	1.57	0.060	0.30
Left dorsal ACC	−5, 14, 42	2.05	0.022	0.40
Right dorsal ACC	5, 14, 42	2.03	0.022	0.39
Left premotor/SMA	−6, −19, 60	1.74	0.042	0.34
Right premotor/SMA	5, −19, 60	1.75	0.042	0.34
Eyes-open beta power band				
Anterior dmPFC	0, 48, 38	2.21	0.015	0.43
Posterior dmPFC	−2, 7, 50	2.72	0.004	0.44
Left rostral ACC	−5, 34, 28	2.13	0.017	0.41
Right rostral ACC	5, 34, 28	2.07	0.020	0.40
Left PCC	−12, −59, 11	1.57	0.060	0.30
Right PCC	10, −58, 14	1.79	0.038	0.35
Left precuneus	−9, −76, 40	1.91	0.029	0.37
Right precuneus	10, −73, 43	1.97	0.003	0.38
Right lateral parietal	54, −47, 15	1.90	0.030	0.37
Left insula	−36, 17, 3	1.65	0.051	0.32
Right insula	38, 19, 0	1.49	0.069	0.29
Left dorsal ACC	−5, 14, 42	2.66	0.004	0.52
Right dorsal ACC	5, 14, 42	2.65	0.005	0.52
Left premotor/SMA	−6, −19, 60	2.83	0.003	0.55
Right premotor/SMA	5, −19, 60	2.76	0.003	0.54

perceived distress and power increases in the default mode and somatomotor networks. On one hand, catastrophizing, along with appraisal processes that ascribe threat-related meaning to experiences, contributes to pain by activating the immune/inflammatory system (Edwards et al., 2008) and the visceromotor (arousal) system (Gianaros and Wager, 2015). Because the visceromotor and skeletomotor systems are coupled systems (Dum et al., 2016), activation of one system is coupled with activation of the other. On the other hand, however—and perhaps explaining the weak *negative* correlation—subjective awareness of distress may enable the activation of top-down cognitive-control mechanisms that help downregulate the allostatic-interoceptive system (Ochsner and Gross, 2005; Aybek et al., 2014). The current data suggest that child and adolescent patients who experienced and reported higher levels of subjective distress may have engaged top-down cognitive-control mechanisms to regulate body state.

Based on the present findings and current models of FND, we might draw inferences about the potential developmental mechanisms that account for a disruption to resting organization of the DMN and SMA. In typical development, slow-wave activity (theta and delta) declines with brain maturation (Knyazev, 2012; Matousek and Petersen, 1973), and this decline is accompanied by the development of an anti-correlation between the default mode and somatomotor networks that helps regulate behaviour and attention (Shannon et al., 2011). In this context, a lack of normally developing organization within and between these networks may disrupt motor control and coordination, and lead to behavioural impulsivity, reactivity, or increased motor readiness (Shannon et al., 2011). As noted earlier, this form of functional organization is associated with a state of increased vigilance and arousal, enables the individual to respond rapidly and automatically to threat, and, under certain conditions (see below), incidentally (we hypothesize) leads to aberrant emotion-motor interactions that generate functional neurological symptoms.

In children/adolescents with FND, this loss of the normal organization within the default mode and somatomotor networks may theoretically occur under three different conditions. The first condition is a *developmental history of ongoing relational stress or emotional trauma* (*psychological stress*), which may modify the typical developmental pathway—in particular, by changing the relationship between the networks as a way of prioritizing and maintaining motor readiness, attention to threat signals, and access to self-protective, reflexive modes of behaviour. Such psychological stressors also prime the brain's innate immune effector cells (glial cells), which hold immunological memory for past stressors, facilitate neural synapse formation and function, and play a key role in network configuration (via synaptic and non-synaptic routes) (Frank et al., 2016; Brenhouse and Schwarz, 2016; von Bernhardi et al., 2016; Rajkowska and Miguel-Hidalgo, 2007; Volterra and Meldolesi, 2005). Against this background—with the neural system already in defensive mode—a further moderate stressor would potentially be sufficient to activate aberrant emotion-motor interactions and generate functional neurological symptoms.

The second condition is a *developmental history of medical illness*—repeated activation of the brain stress systems by infection, inflammation, or repeated physical injuries—which would, as above, change the organization of networks, prime glial cells, and put the neural system into defensive mode. Also as above, a subsequent moderate stressor (physical or psychological) would potentially be sufficient to activate aberrant emotion-motor interactions and generate functional neurological symptoms.

The third condition involves children with a developmental history of relational well-being and interpersonal safety. For such children, *exposure to sudden, uncontrollable stress* (as in contemporary accounts of network reconfiguration in response to uncontrollable stress (Hermans et al., 2011; Arnsten, 2009)) or a *series of cumulative adverse life events* could, in and of itself, induce a functional shift into a defensive state of neural organization, activate aberrant emotion-motor interactions, and generate functional neurological symptoms.

In all three groups, genetic and epigenetic variations that modulate individual differences in the brain's stress response determine the level of vulnerability to stress-induced network reconfiguration. Acquisition of data about genetic/epigenetic vulnerability factors, glial cell function, and network organization during FND illness (vs. periods of

Table 9
Whole brain PRI differences between prepubertal and postpubertal children in the FDN and control groups.

Measure	Mean value prepubertal group (μV2) (n = 22)	Mean value postpubertal group (μV2) (n = 35)	t	df	p-value	Cohen's d effect size
FND group	2.00	1.37	3.40	55	0.001	0.92
Control group	1.53	1.27	1.76	55	0.084	0.47

symptom resolution or remission) will help to fill in details regarding the many different factors that modulate the neural network reorganization that occurs in patients with FND.

Although our spectral-power methodology did not allow us to examine the relationship between the default mode, salience, and somatomotor networks directly, our findings that subjective pain and sympathetic arousal modulated delta increases in the SMA (separate from the default mode and salience networks) are suggestive of altered emotion-motor interactions in our child and adolescent patients with FND. As elegantly stated by Blakemore et al. (2016), the SMA "lie[s] at the intersection of affective-motor processing" (Blakemore et al., 2016) (p230), which means that it is ideally situated as a hub between the default mode and somatomotor networks. The developmental data of Shannon et al. (2011) suggest that when neural networks shift to a more primitive state (that is, down the phylogenetic hierarchy), the SMA comes to work in tandem with (Shannon et al., 2011), rather than antithetically to, the vmPFC, thereby facilitating the translation of threat-related interoceptive signals and negative appraisals into visceromotor and skeletomotor commands (Gianaros and Wager, 2015; Dum et al., 2016). In this way, the SMA may function as a sort of affect-sensitive rheostat, one that is activated by self-relevant, threat-related signals and that modulates the balance between the default mode and somatosensory networks across the range of EEG power frequencies associated with different phylogenetic stages. Importantly, catecholamines released during stress also activate glial cells which regulate levels of network excitability and reset the basal responsiveness (rheostat) of neural circuits (Ding et al., 2013). In this way, power increases in the SMA are likely to reflect complex neuron-glial interactions. In addition, because the SMA is part of the cortico-striato-thalamo-cortical circuit, hyperactivation of the SMA in the resting state may shift these motor circuits into a state of readiness, increasing the probability that aberrant motor responses—in the form of functional neurological symptoms—emerge alongside adaptive ones.

Although power changes in the EEG primarily reflect the summed electrical activities of neurons, the functional activity of neurons is tightly coupled with glial cells (Dong and Greenough, 2004; Zatorre et al., 2012), and glial cells are thought to contribute to the slow-wave power bands of the EEG via several mechanisms. Glial cells have a background voltage—like a single long core conductor (Cohen, 1970)—and show slow voltage fluctuations when they absorb excess potassium ions, dopamine, glutamate, and other neurotransmitters released by neurones (Kofuji and Newman, 2004; Amzica and Steriade, 2000; Amzica et al., 2002; Fields, 2009). Glial cells also have receptors for a range of excitatory and inhibitory neurotransmitters (noradrenalin, glutamate and gamma-aminobutyric acid [GABA]). Neurotransmitter spillage from the neuronal synapse activates these receptors, stimulates a rise in calcium and triggers a calcium wave from glial cell to glial cell—a non-synaptic form of communication—that leads, in turn, to a release of neuroactive substances (gliotransmitters) that excite or depress neuronal aggregates (Fellin et al., 2004; Fields, 2009; Paukert et al., 2014; Kozachkov and Konstantinos, 2017). Glial cell fingers can also move in and out of nerve cell synapses, modulating synapse transmission and neuron activation by controlling the rate of clearance of neurotransmitters (Khakh and Sofroniew, 2015; Fields, 2009). In these ways, glial-cells play a key role in modulating activity in neural networks, including neural networks that mediate increases in arousal and that are involved in the brain's stress response.

In addition to their neuromodulatory functions, glial cells double up as the brain's innate effector immune cells. In this role, glial cells are primed by past stress, they hold immunological memory for past stress, and they activate robustly—secrete pro-inflammatory molecules—in response to subsequent stress (physical or psychological)(Frank et al., 2016). It is now well established that activation of immune-inflammatory cells, including glial cells, is important in the neurobiology of persistent pain (Ji et al., 2016). Because 61–84% of our patients with FND report comorbid pain, we began to consider glial cell involvement in FND (Kozlowska, 2017). To follow up this idea we examined at C-reactive protein levels (a systemic marker of inflammation) in our child and adolescent patients with FND and found CRP titres to be elevated in the low-grade inflammation range (unpublished manuscript in preparation). Our findings of elevated CRP titres led us to contemplate whether glial cell proliferation could potentially explain our recent findings of increased grey matter volumes in the SMA[6] (Kozlowska et al., 2017a). In this context, we theorise that the glial cell activation or proliferation is likely to play an important role maintaining a state of neural activation in the DMN, salience and somatomotor networksin our child and adolescent patients with FND. Coming from a different perspective—the high rate of chronicity in adult patients—Stephenson and Baguley (2018) provide an excellent review of glial-based plasticity mechanisms, and they hypothesize that such glial-based mechanisms explain many of the clinical features of FND (Stephenson and Baguley, 2018).

Our study has a number of limitations. First, our study cohort—like other paediatric cohorts—was made up of participants with mixed FND symptoms. In this context, in contrast to adult studies, it was not possible to subdivide the cohort into "pure" subgroups of children with PNES, or with positive or negative motor symptoms of a particular kind (see Fig. 1). Second, because the topographical map methodology by Giacometti et al. (2014) (Giacometti et al., 2014) is a recent development, the use of electrode clusters as a proxy measure for cortical activation is novel. In this context, we also conducted a whole-brain source-localization analysis using LORETA to confirm that the cortical activations identified by the topographical map overlapped with brain regions identified by the LORETA methodology. Third, since scalp-recorded power values can be influenced by many intra-cortical sources, averaging across different electrodes results in a further blurring of the sources. These are yet-to-be-solved physics problems of EEG recording and analysis. The whole-brain LORETA source localization was run alongside the topographical map methodology in acknowledgment of this problem. Notwithstanding, other studies have also found aberrant activation in both medial frontal regions and medial parietal regions in patients with FND (Vuilleumier and Cojan, 2011). Fourth, our methodology provides no information about the degree to which hyperpolarization of glial cells—which are activated by stress and which modulate the flow of electrical information through neural circuits (Amzica et al., 2002; Fields, 2009)—influenced EEG power increases in our patients. Fifth, the effect sizes for group differences were small to median. That said, our participants were carefully matched by age and sex, and the small to moderate effect sizes were consistently found across both anterior and posterior electrode clusters (cortical regions) and across both methodologies used in the study. Sixth, although our data raise the possibility of changes in the relationship between the DMN, salience network, and SMA, with the shift reflecting a reversion to a more primitive level of neural function, the current methodology did not enable us to test this hypothesis directly. Clarifying the relationship between networks and network nodes is important because Janet's construct of dissociation suggested a disruption of normal connections, whereas the contemporary data in the field of functional neurological symptoms suggest both a weakening of normal connectivity patterns in brain networks—as suggested by Janet (1889); Janet, 1892/1894)—and a strengthening of aberrant ones. In this context the construct of dissociation may need to be revised to take account of findings from contemporary research. Seventh, because our cohort came from regions around the state of New South Wales, large distances precluded us from retesting our patients in the laboratory

[6] When we reported our findings from the structural MRI study with our FND patients Kozlowska K, Griffiths KR, Foster SL, et al. (2017a) Grey matter abnormalities in children and adolescents with functional neurological symptom disorder. *Neuroimage Clin* 15: 306–314. we had not read "Plasticity in grey and white" by Zatorre et al. (2012) and we had not considered the tight functional coupling between neurons, glial cells and data suggesting that gliogenesis is part of experience-learning.

after they recovered. Such retesting would have enabled us to determine whether the functional shift characterized by EEG power increases normalized after the symptoms resolved. Eighth, researchers in the field of FND have identified several "deeper" subcortical and cerebellar neural structures, including the basal ganglia (a motor structure within the cortico-striato-thalamo-cortical circuit) and the cerebellar vermis, as other key are likely to play an important role in aberrant emotion-motor interactions (Blakemore et al., 2016; Vuilleumier, 2014; Barzegaran et al., 2016). Although examination of these "deeper" regions was beyond the limits of our methodology, future studies using functional MRI and high-density EEG (Barzegaran et al., 2016) will be better able to investigate subcortical regions. Finally, this small exploratory study, which looked at a pattern of findings across three brain networks did not have the power to control for multiple comparisons (which would have required a corrected Bonferroni value of $p = 0.006$ for the number of electrode clusters within each power band and for the correlation analyses) (Bender and Lange, 2001).

In conclusion, despite limitations, the current study adds to a growing literature demonstrating that patients with FND show changes in intrinsic resting brain function in regions implicated in arousal, energy regulation, motivation, emotion processing, and self-referential functions and in regions implicated in motor function. Our findings show activation—in electrode clusters that correspond to the default mode network (which is typically activated in the resting state), the salience network (activated by threat stimuli), and somatomotor network (typically deactivated [rather than hyperactivated] in the resting state)—suggesting a defensive brain-body state that prioritizes increased vigilance, increased arousal, changes in pain processing, and increased motor readiness. This state of "motoring in idle" can lead, in turn—in particular circumstances and in particular individuals—to aberrant emotion-motor interactions and functional neurological symptoms.

Acknowledgments

The authors would like to thank all participants who took part in this study. The authors also thank Jenny Peat for her assistance with statistical analyses.

Source of funding and conflicts of interest

This research received no specific grant from any funding agency or from the commercial or not-for-profit sector. Clinical time was funded by Psychological Medicine, The Children's Hospital at Westmead, NSW, Australia. Data acquisition by the Brain Dynamics Centre, Westmead Millennium Institute of Medical Research and University of Sydney Medical School, NSW, Australia. The authors have no conflicts of interest.

Author disclosures

All authors declare that they have no conflict of interest.

Dr. Williams reports personal fees from Humana, personal fees from BlackThorn therapeutics, personal fees from Psyberguide, outside the submitted work.

Dr. Harris reports personal fees from Lundbeck Australia, personal fees from Janssen Cilag, personal fees from Brain Resource, personal fees from Sumitomo Dainippon Pharma, from outside the submitted work.

References

Alper, K.R., John, E.R., Brodie, J., et al., 2006. Correlation of PET and qEEG in normal subjects. Psychiatry Res. 146, 271–282.

AmericanPsychiatric A, 2000. Diagnostic and Statistical Manual of Mental Disorders: DSM-IV-TR. American Psychiatric Association, Washington, DC.

Amzica, F., Steriade, M., 2000. Neuronal and glial membrane potentials during sleep and paroxysmal oscillations in the neocortex. J. Neurosci. 20, 6648–6665.

Amzica, F., Massimini, M., Manfridi, A., 2002. Spatial buffering during slow and paroxysmal sleep oscillations in cortical networks of glial cells in vivo. J. Neurosci. 22, 1042–1053.

Ani, C., Reading, R., Lynn, R., et al., 2013. Incidence and 12-month outcome of non-transient childhood conversion disorder in the UK and Ireland. Br. J. Psychiatry 202, 413–418.

Apazoglou, K., Mazzola, V., Wegrzyk, J., et al., 2017. Biological and perceived stress in motor functional neurological disorders. Psychoneuroendocrinology 85, 142–150.

Arnsten, A.F., 2009. Stress signalling pathways that impair prefrontal cortex structure and function. Nat. Rev. Neurosci. 10, 410–422.

Arnsten, A.F., 2015. Stress weakens prefrontal networks: molecular insults to higher cognition. Nat. Neurosci. 18, 1376–1385.

Aybek, S., Nicholson, T.R., Zelaya, F., et al., 2014. Neural correlates of recall of life events in conversion disorder. JAMA Psychiat. 71, 52–60.

Baddeley, A., Emslie, H., Nimmo-Smith, I., 1993. The spot-the-word test: a robust estimate of verbal intelligence based on lexical decision. Br. J. Clin. Psychol. 32 (Pt 1), 55–65.

Bakvis, P., Roelofs, K., Kuyk, J., et al., 2009a. Trauma, stress, and preconscious threat processing in patients with psychogenic nonepileptic seizures. Epilepsia 50, 1001–1011.

Bakvis, P., Spinhoven, P., Giltay, E.J., et al., 2009b. Basal hypercortisolism and trauma in patients with psychogenic nonepileptic seizures. Epilepsia 51, 752–795.

Barzegaran, E., Joudaki, A., Jalili, M., et al., 2012. Properties of functional brain networks correlate with frequency of psychogenic non-epileptic seizures. Front. Hum. Neurosci. 6, 335.

Barzegaran, E., Carmeli, C., Rossetti, A.O., et al., 2016. Weakened functional connectivity in patients with psychogenic non-epileptic seizures (PNES) converges on basal ganglia. J. Neurol. Neurosurg. Psychiatry 87, 332–337.

Bender, R., Lange, S., 2001. Adjusting for multiple testing–when and how? J. Clin. Epidemiol. 54, 343–349.

von Bernhardi, R., Eugenin-von Bernhardi, J., Flores, B., et al., 2016. Glial cells and integrity of the nervous system. Adv. Exp. Med. Biol. 949, 1–24.

Blakemore, R.L., Sinanaj, I., Galli, S., et al., 2016. Aversive stimuli exacerbate defensive motor behaviour in motor conversion disorder. Neuropsychologia 93, 229–241.

Boord, P.R., Rennie, C.J., Williams, L.M., 2007. Integrating "brain" and "body" measures: correlations between EEG and metabolic changes over the human lifespan. J. Integr. Neurosci. 6, 205–218.

Brenhouse, H.C., Schwarz, J.M., 2016. Immunoadolescence: neuroimmune development and adolescent behavior. Neurosci. Biobehav. Rev. 70, 288–299.

Buzsaki, G., Draguhn, A., 2004. Neuronal oscillations in cortical networks. Science 304, 1926–1929.

Cohen, M.W., 1970. The contribution by glial cells to surface recordings from the optic nerve of an amphibian. J. Physiol. 210, 565–580.

Cohen, R.A., Hitsman, B.L., Paul, R.H., et al., 2006. Early life stress and adult emotional experience: an international perspective. Int. J. Psychiatry Med. 36, 35–52.

Craig, A.D., 2011. Significance of the insula for the evolution of human awareness of feelings from the body. Ann. N. Y. Acad. Sci. 1225, 72–82.

Ding, F., O'Donnell, J., Thrane, A.S., et al., 2013. alpha1-adrenergic receptors mediate coordinated Ca2+ signaling of cortical astrocytes in awake, behaving mice. Cell Calcium 54, 387–394.

Dong, W.K., Greenough, W.T., 2004. Plasticity of nonneuronal brain tissue: roles in developmental disorders. Ment. Retard. Dev. Disabil. Res. Rev. 10, 85–90.

Dum, R.P., Levinthal, D.J., Strick, P.L., 2016. Motor, cognitive, and affective areas of the cerebral cortex influence the adrenal medulla. Proc. Natl. Acad. Sci. U. S. A. 113, 9922–9927.

Edwards, R.R., Kronfli, T., Haythornthwaite, J.A., et al., 2008. Association of catastrophizing with interleukin-6 responses to acute pain. Pain 140, 135–144.

Fellin, T., Pascual, O., Gobbo, S., et al., 2004. Neuronal synchrony mediated by astrocytic glutamate through activation of extrasynaptic NMDA receptors. Neuron 43, 729–743.

Fields, R.D., 2009. The other brain. In: The Scientific and Medical Breakthoughs That Will Heal our Brains and Revoluationize our Health. Simon & Schuster, New York.

Frank, M.G., Weber, M.D., Watkins, L.R., et al., 2016. Stress-induced neuroinflammatory priming: a liability factor in the etiology of psychiatric disorders. Neurobiol. Stress 4, 62–70.

Fried, I., Katz, A., McCarthy, G., et al., 1991. Functional organization of human supplementary motor cortex studied by electrical stimulation. J. Neurosci. 11, 3656–3666.

Giacometti, P., Perdue, K.L., Diamond, S.G., 2014. Algorithm to find high density EEG scalp coordinates and analysis of their correspondence to structural and functional regions of the brain. J. Neurosci. Methods 229, 84–96.

Gianaros, P.J., Wager, T.D., 2015. Brain-body pathways linking psychological stress and physical health. Curr. Dir. Psychol. Sci. 24, 313–321.

Gordon, E.M., Laumann, T.O., Adeyemo, B., et al., 2016. Generation and evaluation of a cortical area Parcellation from resting-state correlations. Cereb. Cortex 26, 288–303.

Gratton, G., Coles, M.G., Donchin, E., 1983. A new method for off-line removal of ocular artifact. Electroencephalogr. Clin. Neurophysiol. 55, 468–484.

Haggard, P., 2008. Human volition: towards a neuroscience of will. Nat. Rev. Neurosci. 9, 934–946.

Hagmann, P., Cammoun, L., Gigandet, X., et al., 2008. Mapping the structural core of human cerebral cortex. PLoS Biol. 6, e159.

Hatch, A., Madden, S., Kohn, M.R., et al., 2010. In first presentation adolescent anorexia nervosa, do cognitive markers of underweight status change with weight gain following a refeeding intervention? Int. J. Eat. Disord. 43, 295–306.

Hermans, E.J., van Marle, H.J., Ossewaarde, L., et al., 2011. Stress-related noradrenergic activity prompts large-scale neural network reconfiguration. Science 334,

1151–1153.
Jackson, J.H., 1884. The Croonian lectures on evolution and dissolution of the nervous system. Br. Med. J. 52, 591–593.
Janet, P., 1889. L'Automatisme Psychologique. Alcan, Paris.
Janet, P., 1892/1894. État mental des hysteriques. Rueff, Paris.
Janig, W., Habler, H.J., 2000. Sympathetic nervous system: contribution to chronic pain. Prog. Brain Res. 129, 451–468.
Ji, R.R., Chamessian, A., Zhang, Y.Q., 2016. Pain regulation by non-neuronal cells and inflammation. Science 354, 572–577.
Jurysta, F., van de Borne, P., Migeotte, P.F., et al., 2003. A study of the dynamic interactions between sleep EEG and heart rate variability in healthy young men. Clin. Neurophysiol. 114, 2146–2155.
Khakh, B.S., Sofroniew, M.V., 2015. Diversity of astrocyte functions and phenotypes in neural circuits. Nat. Neurosci. 18, 942–952.
Kleckner, I.R., Zhang, J., Touroutoglou, A., et al., 2017. Evidence for a large-scale brain system supporting Allostasis and Interoception in humans. Nat. Hum. Behav. 1.
Knyazev, G.G., 2007. Motivation, emotion, and their inhibitory control mirrored in brain oscillations. Neurosci. Biobehav. Rev. 31, 377–395.
Knyazev, G.G., 2012. EEG delta oscillations as a correlate of basic homeostatic and motivational processes. Neurosci. Biobehav. Rev. 36, 677–695.
Knyazev, G.G., Savostyanov, A.N., Bocharov, A.V., et al., 2017. Effortful control and resting state networks: a longitudinal EEG study. Neuroscience 346, 365–381.
Knyazeva, M.G., Jalili, M., Frackowiak, R.S., et al., 2011. Psychogenic seizures and frontal disconnection: EEG synchronisation study. J. Neurol. Neurosurg. Psychiatry 82, 505–511.
Kofuji, P., Newman, E.A., 2004. Potassium buffering in the central nervous system. Neuroscience 129, 1045–1056.
Kozachkov, L., Konstantinos, P.M., 2017. The Causal Role of Astrocytes in Slow-Wave Rhythmogenesis: a Computational Modelling Study. (arXiv preprint arXiv:1702.03993).
Kozlowska, K., 2017. A stress-system model for functional neurological symptoms. J. Neurol. Sci. 383, 151–152.
Kozlowska, K., Williams, L.M., 2010. Self-protective Organization in Children with conversion symptoms: a cross-sectional study looking at psychological and biological correlates. Mind Brain J. Psychiatry 1, 43–57.
Kozlowska, K., Nunn, K.P., Rose, D., et al., 2007. Conversion disorder in Australian pediatric practice. J. Am. Acad. Child Adolesc. Psychiatry 46, 68–75.
Kozlowska, K., Scher, S., Williams, L.M., 2011. Patterns of emotional-cognitive functioning in pediatric conversion patients: implications for the conceptualization of conversion disorders. Psychosom. Med. 73, 775–788.
Kozlowska, K., Brown, K.J., Palmer, D.M., et al., 2013. Specific biases for identifying facial expression of emotion in children and adolescents with conversion disorders. Psychosom. Med. 75, 272–280.
Kozlowska, K., Palmer, D.M., Brown, K.J., et al., 2015a. Reduction of autonomic regulation in children and adolescents with conversion disorders. Psychosom. Med. 77, 356–370.
Kozlowska, K., Palmer, D.M., Brown, K.J., et al., 2015b. Conversion disorder in children and adolescents: a disorder of cognitive control. J. Neuropsychol. 9, 87–108.
Kozlowska, K., Griffiths, K.R., Foster, S.L., et al., 2017a. Grey matter abnormalities in children and adolescents with functional neurological symptom disorder. Neuroimage Clin. 15, 306–314.
Kozlowska, K., Melkonian, D., Spooner, C.J., et al., 2017b. Cortical arousal in children and adolescents with functional neurological symptoms during the auditory oddball task. Neuroimage Clin. 13, 228–236.
van der Kruijs, S.J., Bodde, N.M., Vaessen, M.J., et al., 2012. Functional connectivity of dissociation in patients with psychogenic non-epileptic seizures. J. Neurol. Neurosurg. Psychiatry 83, 239–247.
van der Kruijs, S.J., Jagannathan, S.R., Bodde, N.M., et al., 2014. Resting-state networks and dissociation in psychogenic non-epileptic seizures. J. Psychiatr. Res. 54, 126–133.
Kuner, R., Flor, H., 2017. Structural plasticity and reorganisation in chronic pain. Nat. Rev. Neurosci. 18, 20–30.
Lovibond, S.H., Lovibond, P.F., 1995. Manual for the Depression Anxiety Stress Scale. The Psychological Foundation of Australia, Inc., Sydney.
MacLean, P.D., 1990. The Triune Brain in Evolution: Role in Paleocerebral Functions. Plenum Press, New York.
Matousek, M., Petersen, I., 1973. Automatic evaluation of EEG background activity by means of age-dependent EEG quotients. Electroencephalogr. Clin. Neurophysiol. 35, 603–612.
McEwen, B.S., Gianaros, P.J., 2011. Stress- and allostasis-induced brain plasticity. Annu. Rev. Med. 62, 431–445.
Menon, V., Uddin, L.Q., 2010. Saliency, switching, attention and control: a network model of insula function. Brain Struct. Funct. 214, 655–667.
Mesulam, M.M., 1998. From sensation to cognition. Brain 121 (Pt 6), 1013–1052.
Milligan, E.D., Watkins, L.R., 2009. Pathological and protective roles of glia in chronic pain. Nat. Rev. Neurosci. 10, 23–36.
Mittelbronn, M., Dietz, K., Schluesener, H.J., et al., 2001. Local distribution of microglia in the normal adult human central nervous system differs by up to one order of magnitude. Acta Neuropathol. 101, 249–255.
Nachev, P., Kennard, C., Husain, M., 2008. Functional role of the supplementary and pre-supplementary motor areas. Nat. Rev. Neurosci. 9, 856–869.
Nagata, K., Tagawa, K., Hiroi, S., et al., 1989. Electroencephalographic correlates of blood flow and oxygen metabolism provided by positron emission tomography in patients with cerebral infarction. Electroencephalogr. Clin. Neurophysiol. 72, 16–30.
Nijenhuis, E.R., Spinhoven, P., Vanderlinden, J., et al., 1998. Somatoform dissociative symptoms as related to animal defensive reactions to predatory imminence and injury. J. Abnorm. Psychol. 107, 63–73.
Ochsner, K.N., Gross, J.J., 2005. The cognitive control of emotion. Trends Cogn. Sci. 9, 242–249.
Patrick, J., Dyck, M., Bramston, P., 2010. Depression anxiety stress scale: is it valid for children and adolescents? J. Clin. Psychol. 66, 996–1007.
Paukert, M., Agarwal, A., Cha, J., et al., 2014. Norepinephrine controls astroglial responsiveness to local circuit activity. Neuron 82, 1263–1270.
Puzzo, I., Cooper, N.R., Vetter, P., et al., 2010. EEG activation differences in the pre-motor cortex and supplementary motor area between normal individuals with high and low traits of autism. Brain Res. 1342, 104–110.
Raichle, M.E., 2015. The brain's default mode network. Annu. Rev. Neurosci. 38, 433–447.
Raichle, M.E., MacLeod, A.M., Snyder, A.Z., et al., 2001. A default mode of brain function. Proc. Natl. Acad. Sci. U. S. A. 98, 676–682.
Rajkowska, G., Miguel-Hidalgo, J.J., 2007. Gliogenesis and glial pathology in depression. CNS Neurol. Disord. Drug Targets 6, 219–233.
Schlereth, T., Birklein, F., 2008. The sympathetic nervous system and pain. NeuroMolecular Med. 10, 141–147.
Seeley, W.W., Menon, V., Schatzberg, A.F., et al., 2007. Dissociable intrinsic connectivity networks for salience processing and executive control. J. Neurosci. 27, 2349–2356.
Shannon, B.J., Raichle, M.E., Snyder, A.Z., et al., 2011. Premotor functional connectivity predicts impulsivity in juvenile offenders. Proc. Natl. Acad. Sci. U. S. A. 108, 11241–11245.
Smith, S.M., Fox, P.T., Miller, K.L., Glahn, D.C., Fox, P.M., Mackay, C.E., et al., 2009. Correspondence of the brain's functional architecture during activation and rest. Proc. Natl. Acad. Sci. U. S. A. 106, 13040e5.
Stephenson, C.P., Baguley, I.J., 2018. Functional neurological symptom disorder (conversion disorder): a role for microglial-based plasticity mechanisms? Med. Hypotheses.
Tabachnick, B.G., Fidell, L.S., 2007. Using Multivariate Statistics. Pearson Education, New York.
Teves, D., Videen, T.O., Cryer, P.E., et al., 2004. Activation of human medial prefrontal cortex during autonomic responses to hypoglycemia. Proc. Natl. Acad. Sci. U. S. A. 101, 6217–6221.
Touroutoglou, A., Bickart, K.C., Barrett, L.F., et al., 2014. Amygdala task-evoked activity and task-free connectivity independently contribute to feelings of arousal. Hum. Brain Mapp. 35, 5316–5327.
Umesh, S., Tikka, S.K., Goyal, N., et al., 2017. Aberrant gamma band cortical sources and functional connectivity in adolescents with psychogenic non-epileptic seizures: a preliminary report. Psychiatry Res. 247, 51–54.
Vachon-Presseau, E., Centeno, M.V., Ren, W., et al., 2016. The emotional brain as a predictor and amplifier of chronic pain. J. Dent. Res. 95, 605–612.
Volterra, A., Meldolesi, J., 2005. Astrocytes, from brain glue to communication elements: the revolution continues. Nat. Rev. Neurosci. 6, 626–640.
Voon, V., 2014. Functional neurological disorders: imaging. Neurophysiol. Clin. 44, 339–342.
Voon, V., Brezing, C., Gallea, C., et al., 2010. Emotional stimuli and motor conversion disorder. Brain 133, 1526–1536.
Vuilleumier, P., 2014. Brain circuits implicated in psychogenic paralysis in conversion disorders and hypnosis. Neurophysiol. Clin. 44, 323–337.
Vuilleumier, P., Cojan, Y., 2011. Functional brain-imaging of psychogenic paralysis during conversion and hypnosis. In: Hallett, M., Cloninger, C., Fahn, S. (Eds.), Psychogenic Movement Disorders and Other Conversion Disorders. Cambridge University Press, Cambridge, pp. 143–159.
Wang, X., Ongur, D., Auerbach, R.P., et al., 2016. Cognitive vulnerability to major depression: view from the intrinsic network and cross-network interactions. Harv. Rev. Psychiatry 24, 188–201.
Wegrzyk, J., Kebets, V., Richiardi, J., et al., 2017. Identifying motor functional neurological disorder using resting-state functional connectivity. Neuroimage Clin. 17, 163–168.
Williams, L.M., 2017. Defining biotypes for depression and anxiety based on large-scale circuit dysfunction: a theoretical review of the evidence and future directions for clinical translation. Depress. Anxiety 34, 9–24.
Xue, Q., Wang, Z.Y., Xiong, X.C., et al., 2013. Altered brain connectivity in patients with psychogenic non-epileptic seizures: a scalp electroencephalography study. J. Int. Med. Res. 41, 1682–1690.
Zatorre, R.J., Fields, R.D., Johansen-Berg, H., 2012. Plasticity in gray and white: neuroimaging changes in brain structure during learning. Nat. Neurosci. 15, 528–536.
Zhang, S., Ide, J.S., Li, C.S., 2012. Resting-state functional connectivity of the medial superior frontal cortex. Cereb. Cortex 22, 99–111.